New insights into the Late Ordovician magmatism in the Eastern Pyrenees: U–Pb SHRIMP zircon data from the Canigó massif

Josep M. Casas [a,*], Pedro Castiñeiras [b], Marina Navidad [b], Montserat Liesa [c], Jordi Carreras [d]

[a] Departament de Geodinàmica i Geofísica-Institut de recerca GEOMODELS, Universitat de Barcelona, Martí i Franquès s/n, Barcelona, 08028, Spain
[b] Departamento de Petrología y Geoquímica-Instituto de Geología Económica, (CSIC) Universidad Complutense de Madrid, José Antonio Novais 2, Madrid, 28040, Spain
[c] Departament de Geoquímica, Petrologia i Prospecció Geològica, Universitat de Barcelona, Martí i Franquès s/n, Barcelona, 08028, Spain
[d] Departament de Geologia, Universitat Autònoma de Barcelona, Bellaterra (Cerdanyola del Vallès), 08193, Spain

Keywords:
Pre-Variscan
Late Ordovician magmatism
SHRIMP geochronology
U–Pb zircon
Canigó massif
Eastern Pyrenees

A B S T R A C T

New geochronological data from the Canigó massif (Eastern Pyrenees) using U–Pb SIMS on zircon provide evidence of the existence of a late Ordovician (456–446 Ma) plutonic event that emplaced granitic and dioritic bodies into a late Neoproterozoic–Early Paleozoic metasedimentary series. These are the first geochronological data documenting this magmatic episode in the Pyrenees, which is coeval with synsedimentary volcanism and normal fault development in rocks of the Upper Ordovician. This Late Ordovician magmatic event postdates a ?Middle Ordovician compressional episode recorded in the pre-Upper Ordovician sequence, and is distinct from an Early Ordovician magmatic event that gave rise to the protoliths of large gneissic bodies cropping out in the Pyrenees. This evolution argues against a continuous extensional regime related to the opening of the Rheic or the Rheic and Paleotethys oceans in this segment of the Northern Gondwana margin during the Ordovician and Silurian.

1. Introduction

Orthogneiss bodies are widespread in the pre-Upper Ordovician sequences of the Eastern Pyrenees. Recent geochronological data show that the protoliths of some of these gneisses emplaced into the lowermost part of the metasedimentary series (the Port gneiss in the Cap de Creus massif and the Mas Blanc gneiss in the Roc de Frausa massif, Fig. 1), are related to an episode of Late Neoproterozoic–Early Cambrian magmatism (553 ± 4 Ma and 560 ± 7 Ma respectively, Castiñeiras et al., 2008a). Younger, Early–mid-Ordovician magmatism (477–460 Ma, Cocherie et al., 2005; Castiñeiras et al., 2008a; Liesa et al., in press) emplaced the protoliths of large laccolithic gneiss bodies into the middle part of the pre-Upper Ordoviciansuccession. These gneisses crop out at the core of a series of antiformal massifs (Canigó, Roc de Frausa and Albera gneisses, Fig. 1). This Early Ordovician magmatism, which is related to the break-up of the northern Gondwanan margin, is widespread in other areas of the European Variscides (Vialette et al., 1987; Pin and Marini, 1993; Valverde-Vaquero and Dunning, 2000; Helbing and Tiepolo, 2005; Talavera et al., 2008; Oggiano et al., 2010-this issue. Yet other gneissic and metabasite bodies have not been dated or have yielded inconclusive ages. This is the case for the Casemí and Cadí gneisses that crop out in the central part of the Canigó massif and constitute the deepest metaplutonic rocks of the Eastern Pyrenees (Figs. 2–4). In this paper, we present new geochronological data using U–Pb SIMS (SHRIMP) on zircon obtained from four samples of the Casemí and Cadí gneisses in the Canigó massif (Fig. 4). The data document a well-defined Late Ordovician magmatic event that gave rise to the intrusion of granitic and dioritic bodies into the lower part of the pre-Upper Ordovician sequence. We discuss the significance of this event in relation to Upper Ordovician volcanism and Ordovician deformational events in the Pyrenees.

2. Geological setting

The Canigó massif is an E–W oriented antiformal structure that reflects the superposition of two late Variscan fold systems and/or the development of a fold linked to the underlying Alpine thrust (Figs. 2 and 3). As in the rest of the Eastern Pyrenees, the Variscan rocks were uplifted in response to Oligocene–Miocene extensional tectonics. A set of NE–SW and NW–SE normal faults (Fontboté and Guitard, 1958) (Figs. 2 and 3) were active during Oligocene–Neogene times and some of them were reactivated during the Pliocene (Maurel et al., 2002). The normal motion on these faults exerted a strong influence on topography, favouring the outcrop of the lowermost materials. For instance, the Marialles and Mentet–Fillols faults cut across the central part of the massif and account for the outcrop of the series underlying the Canigó gneiss in this part of the massif (Figs. 2 and 3). As a result, one of the most complete pre-Upper Ordovician

* Corresponding author. Tel.: +34 934021388.
E-mail address: casas@ub.edu (J.M. Casas).

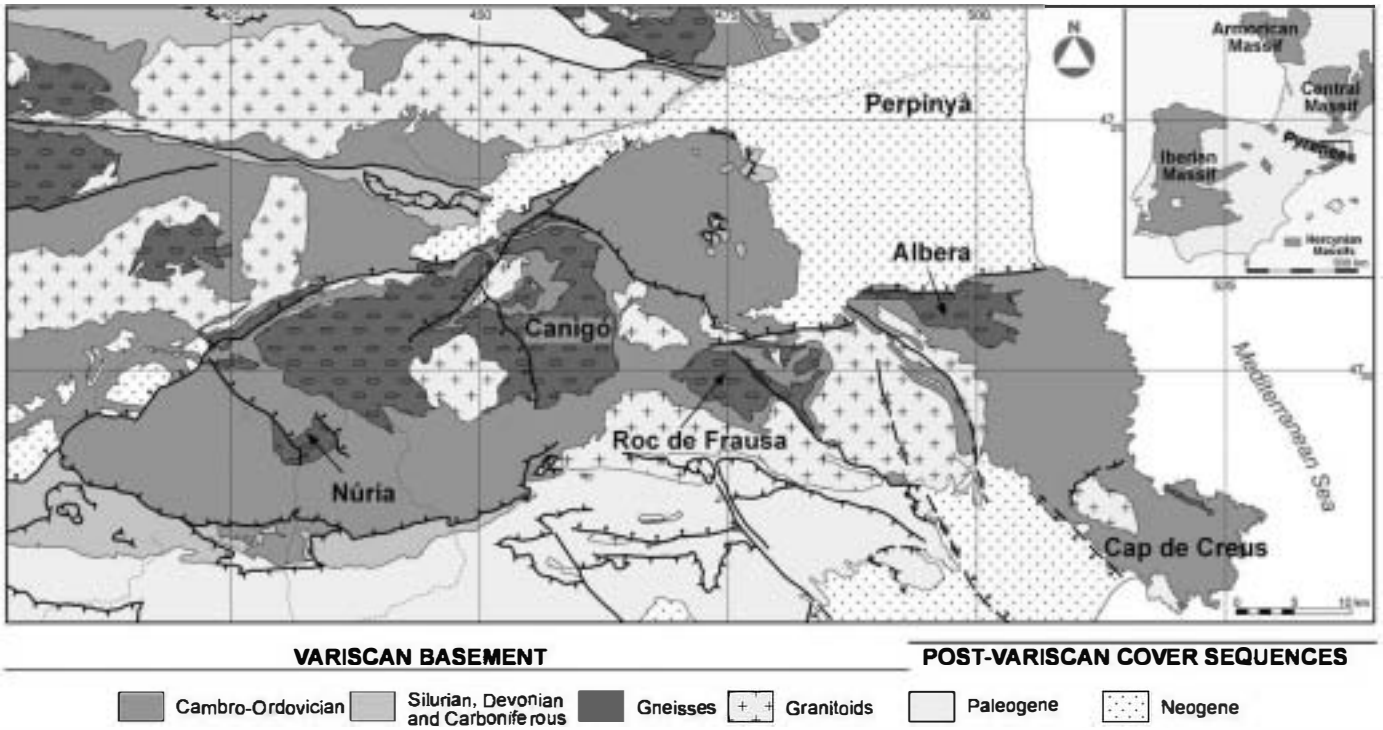

Fig. 1. Geological sketch map of the Variscan basement and cover sequences in the Eastern Pyrenees.

sequences of the Pyrenees is preserved in the Canigó massif (Fig. 1). This sequence is divided into two parts by the Canigó gneiss, which is a thick (3000 m) granitic orthogneiss body (Figs. 2–4).

The sequence overlying the gneiss is mainly composed of metapelites (up to 3000 m thick) interbedded with numerous layers of metabasites, rhyodacitic tuffs, marbles, quartzites and calc-silicate rocks. The age of this sequence is a matter of debate because of its unfossiliferous character, although trace fossils have recently been found. A mid- to Late Cambrian (Abad, 1987; Laumonier, 1988) or Late Cambrian to Early Ordovician age (Guitard et al., 1998) has been proposed for its upper part. Recent radiometric dating (U–Pb SIMS on zircon) of an interlayered metatuff has yielded Late Neoproterozoic–Cambrian ages (581 and

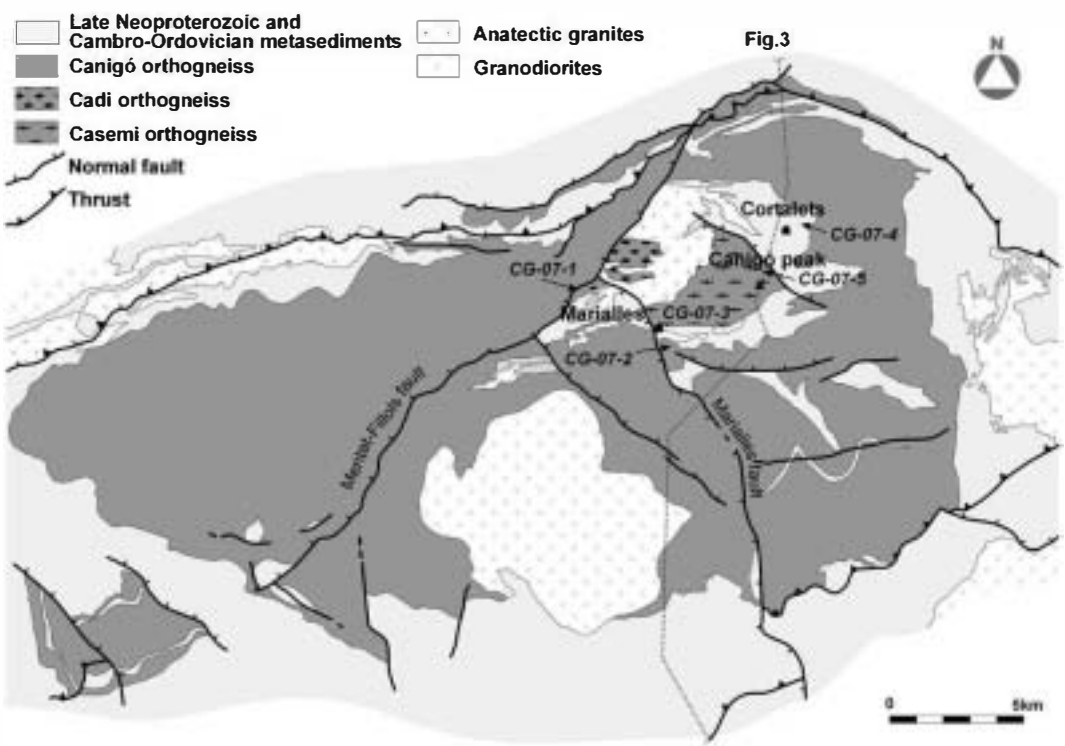

Fig. 2. Geological map of the Canigó massif showing sample locations, the location of the Marialles and Cortalets refuges, and the cross-section line illustrated in Fig. 3. Modified after Guitard (1970), Santanach (1972), Casas (1984), and Ayora and Casas (1986).

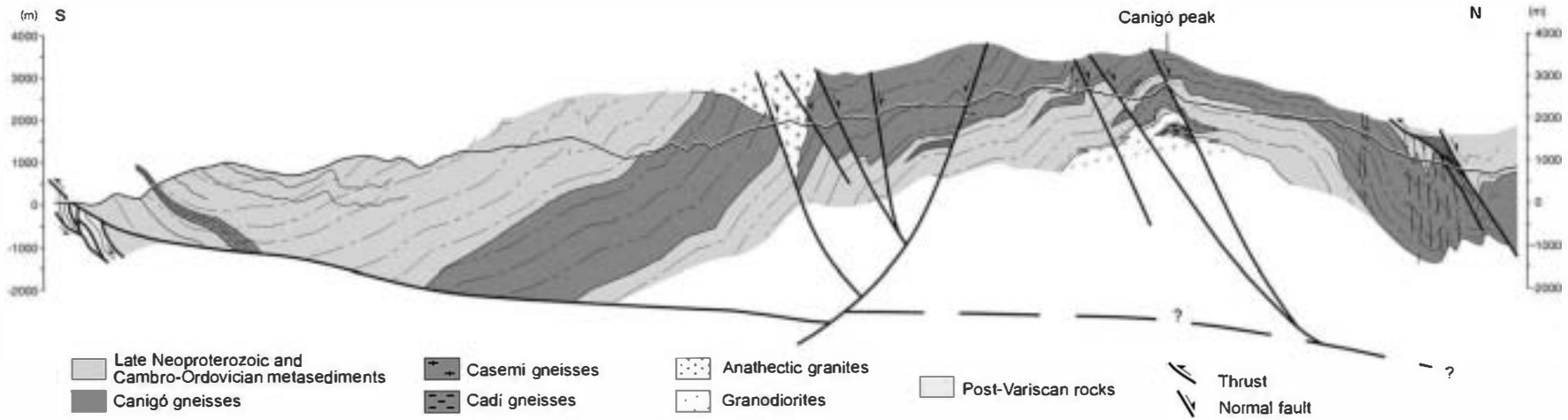

Fig. 3. Cross section through the Canigó massif modified after Alias et al. (2000). See Fig. 2 for location.

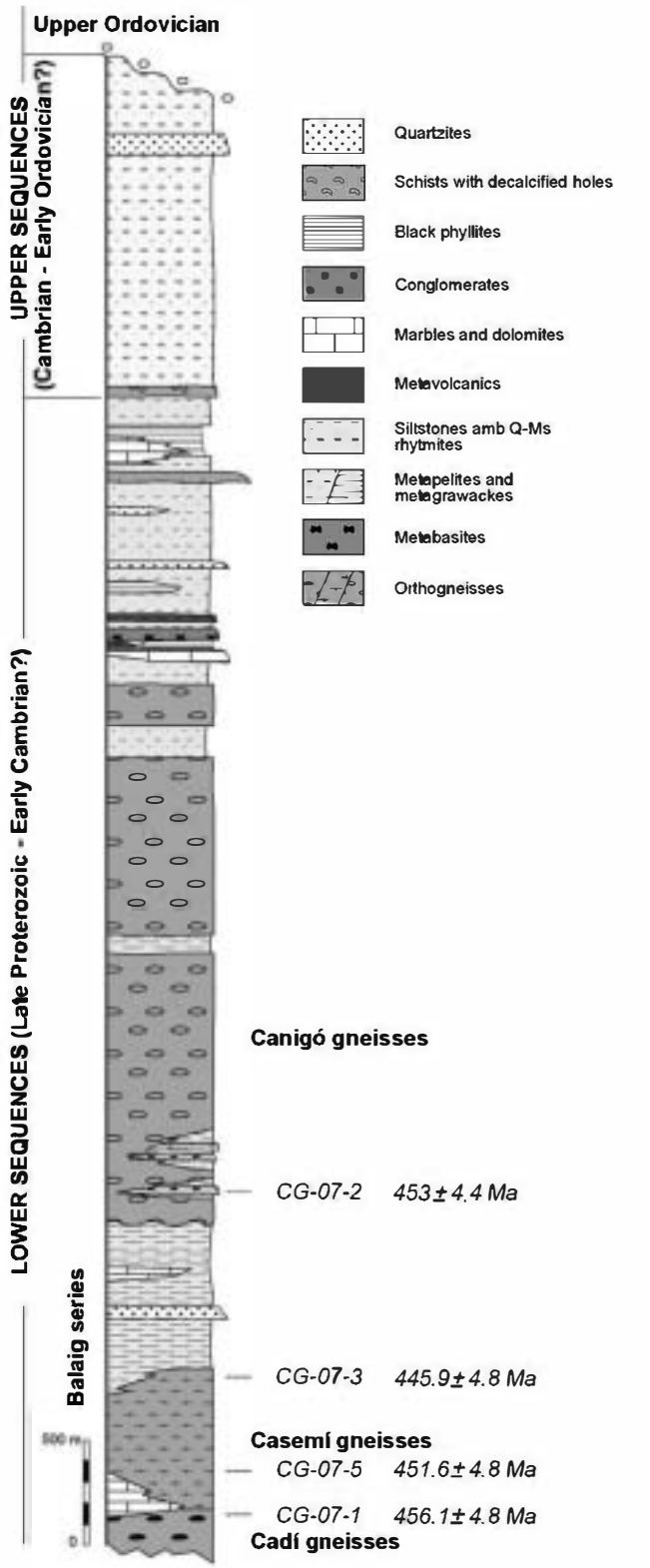

Fig. 4. Synoptic stratigraphic column of the pre-Upper Ordovician rocks of the Canigó massif showing sample locations. Data modified after Guitard (1970), Santanach (1972), Casas (1984), and Ayora and Casas (1986).

540 Ma) for the middle part of the succession (Cocherie et al., 2005 and Castiñeiras et al., 2008a respectively). U–Pb age data have also shown that the Canigó gneiss is derived from an Early Ordovician granite intruded into the pre-Upper Ordovician metasedimentary sequence (Cocherie et al., 2005). These data preclude a Cadomian granitic basement protolith for the Canigó gneiss, thereby invalidating the basement-cover model previously proposed by Guitard (1970) (see discussion in Laumonier et al., 2004).

The series underlying the gneiss (Balaig series, Guitard, 1953) is up to 1500 m thick and comprises a succession of mica schists with marble, quartzite and metabasite intercalations. This series is lithologically and chemically very similar to the lower part of the Late Neoproterozoic–pre-Upper Ordovician metasedimentary sequence, favouring Guitard's (1970) interpretation of the Balaig series as the equivalent of the lowermost part of this sequence repeated under the Canigó gneisses by means of a large recumbent fold. Geochronological and regional data, however, refute this model (see discussion in Laumonier et al., 2004 and Castiñeiras et al., 2008a) and establish the Balaig mica schists and underlying Cadí gneiss as the deepest rocks in the Canigó massif. The age of the Balaig series remains unresolved, although an age slightly older than the plutonic rocks in the lower part in equivalent series in the Cap de Creus and Roc de Frausa massifs seems likely (older than ?600 Ma, Castiñeiras et al., 2008a).

The Casemí gneiss (Guitard, 1970) constitutes the most remarkable metaigneous intercalation in the Balaig series (Fig. 4). It is a laccolithic body mainly made up of fine-grained biotitic and amphibolic granitic gneisses up to 1000 m thick that form the highest peaks of the massif. According to Guitard (1970), these gneisses were derived from an acidic volcanic body interlayered within the mica schists. Delaperrière and Soliva (1992) obtained an age of 425 ± 18 Ma (Wenlock) for the Casemí gneiss based on single-crystal Pb evaporation method on zircon, which favours an intrusive origin for the protolith of this gneiss. However, this Silurian age seems to be unrelated to any other magmatic occurrence in the pre-Variscan rocks of the Pyrenees.

The deepest rocks in the Canigó massif are the Cadí gneisses (Guitard, 1970), which crop out in the footwall of the Mentet–Fillols fault underlying the Balaig series (Figs. 2–4). They are granitic augen gneisses with lithological characteristics similar to those of the Canigó gneisses. No geochronological data are presently available and the interpretation of Guitard (1970) that the Cadí gneisses are a tectonic repetition of the Canigó gneisses under the Balaig series is mainly based on their similar lithological characteristics.

The whole succession was affected by polyphase Variscan deformation (late Visean to Serpukhovian) accompanied by high temperature–low pressure metamorphism (Guitard, 1970; Zwart, 1979). Syn- to late-orogenic (Moscovian–Kasimovian) granitoids intruded mainly into the upper levels of the succession, producing local contact metamorphism (Autran et al., 1970).

3. SHRIMP U–Pb zircon geochronology

Five samples were collected for U–Pb zircon analysis from the lower sequences in the central part of the Canigó massif (Figs. 2 and 4). Sample CG-07-1 was collected from the Cadí gneiss in the footwall of the Mentet–Fillols fault (UTM: x448973, y4706647, z1140 m). The sample has a gneissic–mylonitic texture with feldspar porphyroclasts. K feldspar is more abundant than plagioclase, which is altered to sericite. Matrix minerals are recrystallized quartz, biotite, chlorite and epidote from biotite, rutile and opaque ore.

The Casemí gneiss was sampled near the Marialles refuge (CG-07-3, UTM: x451605, y4705755, z1724 m) and at the base of the Canigó peak (CG-07-5, UTM: x455550, y4707616, z2445 m). Sample CG-07-03 is a homeoblastic foliated gneiss, rich in quartz and amoeboid feldspar. Mica is scarce, and muscovite is more abundant than biotite. Epidote and opaque ore are also present. Sample CG-07-05 is also a homeoblastic gneiss, with feldspar porphyroclasts and matrix made up of quartz, biotite, hornblende, pyramidal zircon, allanite and opaque ore.

Additionally, two samples of metabasite interlayered in the Balaig mica schists were collected. Sample CG-07-2 (UTM: x451675, y4704840, z1800 m) was collected near the Marialles refuge and is an amphibolite (metadiorite) comprising amphibole, hornblende,

plagioclase and quartz. Biotite is scarce and accessory minerals are titanite and opaque ore. The fabric is foliated and lineated and grain size is homogeneous. Sample CG-07-4 was collected near the Cortalets refuge (UTM: *x*457039, *y*4709327, *z*1926 m) and is a well-foliated amphibolite made up of green amphibole, zoisite, titanite and scarce chlorite and plagioclase.

3.1. Zircon description

Zircon from the collected samples was isolated at the Universidad Complutense (Madrid) using a combination of gravimetric (Wilfleytable and methylene iodide) and magnetic (Frantz isodynamic separator) techniques.

Zircon crystals from the Cadí gneiss (sample CG-07-1) are colourless to pale yellow prisms with breadth-to-length ratios between 1:2 and 1:3, well-developed composite pyramidal faces, and are virtually free of inclusions. Under cathodoluminescence (CL), they exhibit clear core-rim structures with abundant inherited cores rimmed by magmatic oscillatory zones (Fig. 5a).

Zircon grains from one of the Casemí gneiss samples (CG-07-3) are broken colourless prisms with simple pyramids, irregular faces and common inclusions. Under CL, they are luminescent, with some grains displaying broad homogeneous or sector zoned central areas surrounded by finely zoned oscillatory bands; in other cases, the whole grain has an oscillatory zoning (Fig. 5b). In the other Casemí gneiss sample (CG-07-5), zircons are small, stubby colourless to deep brown grains with pitted faces and some inclusions. They are moderately luminescent with oscillatory zoning (Fig. 5c).

The metabasite interlayered in the Balaig series (sample CG-07-2) corresponds to a microdiorite. Zircon grains in this sample are large, broken, colourless to brownish prisms with tetragonal pyramids and irregular or pitted faces. There are abundant inclusions of major minerals. They are poorly luminescent and display homogeneous central areas surrounded by hazy oscillatory zones (Fig. 5d). The other metabasite sample collected in the Balaig series (sample CG-07-4) yielded no zircon crystals.

3.2. Analytical methods

About 35 representative zircon grains per sample were handpicked under a binocular microscope and mounted in parallel rows on a double-sided adhesive together with some chips of zircon standard R33 (Black et al., 2004). After being set in epoxy resin, the zircons were ground down to expose their central portions by using 1500 grit wet sandpaper, and polished with 6 μm and 1 μm diamond abrasive on a lap wheel. Prior to isotopic analysis, the internal structure, inclusions, fractures and physical defects were identified with transmitted and reflected light on a petrographic microscope, and with cathodoluminescence on a JEOL JSM 5600 electron microscope housed at SUMAC (Stanford-US Geological Survey micro analytical centre). After the analysis, secondary electron images were taken to locate the exact position of the spots.

U–Th–Pb analyses of zircon were made on the Bay SHRIMP-RG (sensitive high resolution ion microprobe-reverse geometry) jointly operated by the US Geological Survey and Stanford University in the SUMAC facility at Stanford University during a single analytical session on Memorial Day in 2008.

Analytical procedure for zircon dating followed methods described in Williams (1997). Before loading the mount into the source chamber, the sample was thoroughly cleaned by washing it with soap and then soaking the mount in an acid, either EDTA or 1 N HCl, to remove common lead contamination that may have taken place during sample preparation. This cleansing procedure, together with the rastering of the primary beam for 90–120s over the area for analysis before data collection, ensures that any counts found at mass ^{204}Pb are actually Pb from the zircon and not surface contamination. Accordingly, SQUID estimates the Pb composition used for initial Pb corrections of the unknowns using the age of the unknown (instead of the modern Pb composition) and the Stacey and Kramers (1975) model.

The primary oxygen ion beam operated at 6–7 nA and produced a spot with a diameter of ~25 μm and a depth of 1–2 μm for an analysis time of around 11 min. Data for each spot were collected utilizing five-cycle runs through the mass stations. The concentration of U was calibrated using zircon standard CZ3 (550 ppm U, Pidgeon et al., 1995), and isotopic compositions were calibrated against R33 ($^{206}Pb^*/^{238}U = 0.06716$, equivalent to an age of 419 Ma, Black et al., 2004), which was measured every four analyses.

SQUID and Isoplot software (Ludwig, 2002, 2003) were used for data reduction, following the methods described by Williams (1997) and Ireland and Williams (2003).

Ages are based on $^{206}Pb/^{238}U$ ratios corrected for common Pb using the ^{207}Pb method on the assumption that common Pb proceeds from the sample and not from surface contamination. Analytical results are presented in Supplementary Table 1 (available from journal website) and uncorrected ratios are plotted in Fig. 6.

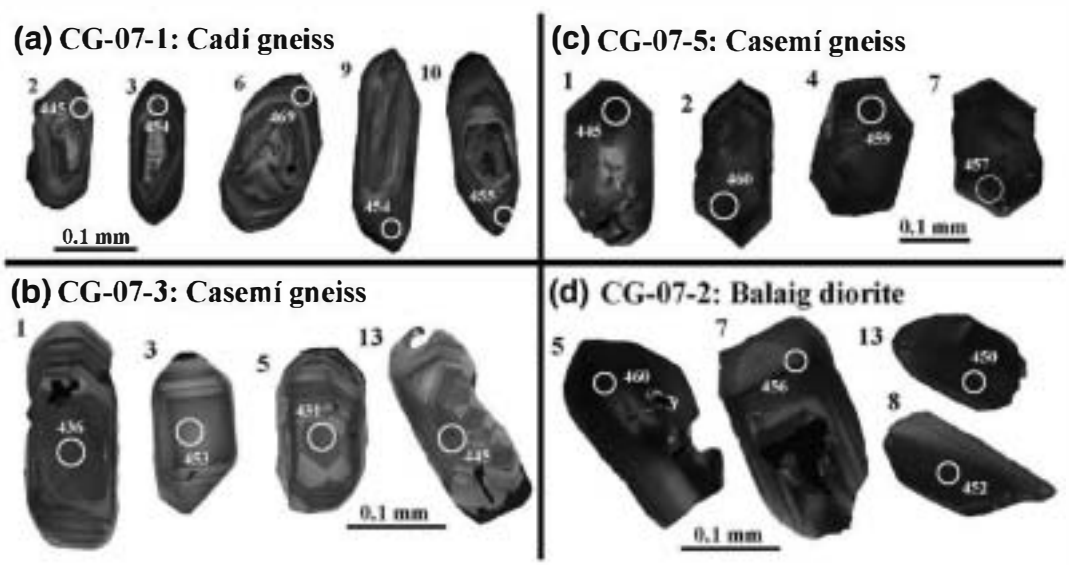

Fig. 5. Cathodoluminescence images of selected zircons: (a) Cadí gneiss (sample CG-07-1); (b) and (c) Casemi gneiss (sample CG-07-3 and CG-07-5), and (d) Balaig microdiorite (sample CG-07-2).

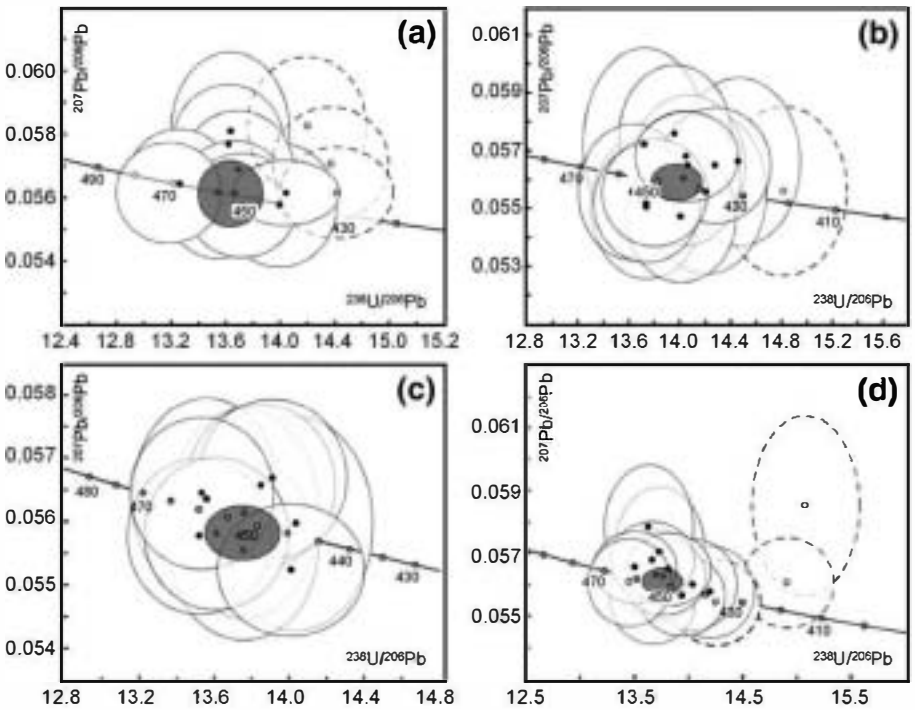

Fig. 6. Tera–Wasserburg plot showing distribution of SHRIMP zircon analyses: (a) Cadí gneiss (sample CG-07-1); (b) and (c) Casemí gneiss (sample CG-07 and CG-07-5), and (d) Balaig microdiorite (sample CG-07-2). Dashed ellipses represent analyses not considered for the concordia age calculation (grey ellipse). Error ellipses are ± 2σ.

3.3. U–Pb results

Concordia ages, *sensu* Ludwig (1998), were calculated for all of the samples, rejecting the outlier young analyses because of the possibility of lead loss. Fourteen zircon grains from the Cadí gneiss (sample CG-07-1) were analyzed, using cathodoluminescence images to target oscillatory zones considered to be magmatic. Ten analyses yielded a concordia age of 456.1 ± 4.8 Ma with a mean square of weighted deviation for concordance and equivalence (MSWD) equal to 1.9 (Fig. 6a). This result is interpreted to be the crystallization age of the igneous protolith.

In sample CG-07-3 from the Casemí gneiss, fourteen zircons were analyzed in magmatic areas with homogeneous, sector or oscillatory zoning. All of the analyses but one yielded a concordia age of 445.9 ± 4.8 Ma (Fig. 6b) with an MSWD of 1.3. In the other Casemí gneiss sample (CG-07-5), ten analyses that targeted oscillatory zones yielded a concordia age of 451.6 ± 4.8 Ma (Fig. 6c) with an MSWD of 1.11. The ages obtained in both Casemí gneiss samples are equivalent within error and they are interpreted to record the crystallization age of the igneous protolith.

In the Balaig microdiorite, sixteen analyses were obtained from magmatic areas in 15 zircon grains. A concordia age of 453 ± 4.4 Ma (MSWD = 1.3) was calculated by pooling together twelve analyses (Fig. 6d), which is interpreted to record the crystallization age of the igneous protolith.

4. Discussion

The new age data show that the Cadí gneiss, Casemí gneiss and microdiorite bodies were intruded into the Balaig series during a Late Ordovician magmatic event (456 to 446 Ma). This age corresponds to the sixth global stage (Katian) of the Ordovician, which is roughly equivalent to upper Caradoc–middle Ashgill in the regional British series division (see Finney, 2005). The data are also the first to document a Late Ordovician magmatic episode in the pre-Upper Ordovician rocks of the Pyrenees. Accordingly, the Cadí and Canigó gneisses, despite being very similar lithologically, were derived from two different plutonic bodies emplaced into the lower part of the pre-Upper Ordovician metasedimentary sequence. It therefore follows that the Canigó massif is the only massif in the Pyrenees in which two Ordovician magmatic events have been recorded: an Early Ordovician event (Canigó gneiss, 467 ± 7 to 477 ± 4 Ma, Cocherie et al., 2005) and a Late Ordovician event (Cadí and Casemí gneisses, 456.1 ± 4.8 and 445.6 ± 4.8 Ma).

Elsewhere in the Pyrenees, an Early Ordovician magmatic event ranging in age from 477 and 467 Ma has been described in the Roc de Frausa (476 ± 5 Ma, Castiñeiras et al., 2008a), the Albera massifs (470 ± 3 Ma, Liesa et al., in press), and the Aston and Hospitalet massifs (470 ± 6 Ma and 472 ± 2 Ma respectively, Denele et al., 2009). Late Cambrian/Early Ordovician ages are also common in the Iberian Massif (Guadarrama orthogneisses: 470 to 480 Ma, Vialette et al., 1987; Cardoso gneiss: 480 ± 2 Ma and La Morcuera gneiss: 477 ± 4 Ma, Valverde-Vaquero and Dunning, 2000; Miranda do Douro gneiss: 483 ± 3 Ma, Bea et al., 2006 and 496 ± 3 Ma, Zeck et al., 2007; Sotosalbos anatectic gneiss: 465 to 480 Ma, Castiñeiras et al., 2008b; Ollo de Sapo Fm., 488 ± 6 and 472 ± 12 Ma, Díez Montes et al., 2010-this issue, among others) and in Sardinia (Lula porhyroid: 474 ± 13 Ma, Helbing and Tiepolo, 2005; metarhyolite and metadacite: 491.7 ± 3.5 Ma to 479.9 ± 2.1 Ma, Oggiano et al., 2010-this issue).

The Cadí and Casemí gneisses, together with the microdiorite bodies, can be regarded as the plutonic equivalent of coeval Late Ordovician volcanic rocks interlayered in the Upper Ordovician sequence of the Pyrenees (Ravier et al., 1975; Robert and Thiebaut 1976; Martí et al., 1986; Calvet et al., 1988), the southern French Massif Central (Marini, 1988), and the Catalan Coastal Ranges (Navidad and Barnolas, 1991; Barnolas and García-Sansegundo, 1992). A detailed description of new geochronological and geochemical data on this Upper Ordovician magmatism in the Pyrenees and the Catalan Coastal Ranges is provided by Navidad et al. (2010-this issue). Late Ordovician ages have also been obtained for magmatic bodies in the southern part of the French Massif Central (Pont de Larn orthogneiss: 456 ± 3 Ma and Gorges d'Heric orthogneiss: 450 ± 6 Ma, Roger et al., 2004), and in Sardinia (Tanaunella orthogneiss: 458 ± 7 Ma and Lodè orthogneiss: 456 ± 14 Ma, Helbing and Tiepolo, 2005). In Sardina, however, the Capo Spartivento gneiss

yields different ages depending on the analytical procedure used: Late Ordovician (449 Ma, Ludwig and Turi, 1989, SIMS data) and Early Ordovician (478 ± 6 Ma, Delaperrière and Lancelot, 1989, U–Pb in zircons). Late Ordovician ages have also been obtained in the Peloritan Range of Sicily for felsic porphyroids (456–452 Ma, Trombetta et al., 2004) and in the Alps, where a 450–460 Ma magmatic event has been reported in the Penninic (Guillot et al., 2002) and Central Swiss Alps (Schaltegger et al., 2003).

In the Pyrenees, this Late Ordovician magmatic episode is coeval with normal fault development affecting the lower part of the Upper Ordovician series, the basal unconformity, and the underlying pre-Upper Ordovician sediments (Casas and Fernández, 2007; Casas and Fernández, 2008; Casas, in press). Between the Early and the Late Ordovician magmatic events, and prior to this episode of normal faulting, a mid-Ordovician folding phase gave rise to NW–SE to N–S metre- to hectometre-scale folds. These folds are not associated with coeval cleavage development or metamorphism, but account for the deformation of the pre-Upper Ordovician sequence and the formation of the Upper Ordovician unconformity (Casas, in press). In the Alps, a mid-Ordovician compressional event has been reported by Zurbriggen et al. (1997) and Handy et al. (1999) in the Sesia Zone, where it is associated with amphibolite facies metamorphism. HP metamorphism in the Aar Massif (468 Ma, Schaltegger et al., 2003) and in the Southern Alps (457 ± 5 Ma, Franz and Romer, 2007) also provides evidence of an Ordovician orogenic cycle subsequently overprinted by Variscan deformation.

By contrast, Late Ordovician magmatic activity is relatively scarce in the rest of the Iberian Massif (see Murphy et al., 2008) and evidence of Ordovician deformations is limited. A mid-Ordovician deformational episode has not been reported and the pre-Variscan compressional episodes that have been described are older than those in Sardinia, the Pyrenees, or the Alps, since they are constrained to the post-mid-Cambrian and pre-Early Arenig (see discussion in Casas, in press). This suggests that the western part of the Northern Gondwana margin (Iberian Massif) evolved differently from the eastern part of the margin (Pyrenees, French Massif Central, Sardinia, Sicily and the Alps) following the Early Ordovician.

The occurrence of a mid-Ordovician tectono-metamorphic event and a Late Ordovician magmatic episode appears to be characteristic of the eastern part of the Northern Gondwanan margin. This supports the evolution described by Stampfli et al. (2002) and von Raumer et al. (2002) who propose that the extensional regime developed during the Late Ordovician resulted from the collapse of a short-lived cordillera that formed during the mid-Ordovician. This cordillera resulted from the amalgamation of volcanic arcs and continental ribbons in a transient mid-Ordovician orogenic pulse (Stampfli et al., 2002; von Raumer et al., 2002), and started to collapse during the Late Ordovician in a setting dominated by Gondwana-directed subduction of a former peri-Gondwanan ocean.

5. Conclusions

Dating of metaigneous rocks of the Canigó massif using U–Pb SHRIMP in zircon documents Late Ordovician ages for the Cadí gneiss (456.6 ± 4.8 Ma), the Casemí gneiss (445.9 ± 4.8 and 451.6 ± 4.8 Ma), and a microdiorite body (453 ± 4.4 Ma) emplaced into the lower part of the pre-Upper Ordovician sequence.

These results refute the previously proposed Silurian age for the Casemí gneiss and link the emplacement of all three bodies to the magmatic event responsible for the Upper Ordovician volcanism recorded in the Pyrenees and the Catalan Coastal Ranges.

This Late Ordovician (456–446 Ma) magmatic event is distinct from the Early Ordovician event that gave rise to the large gneissic bodies (Canigó, Roc de Frausa and Albera gneisses) that form the core of the Eastern Pyrenean massifs. Hence, three different magmatic episodes, Late Neoproterozoic–Early Cambrian, Early Ordovician and Late Ordovician, can be identified in the pre-Silurian rocks of the Eastern Pyrenees.

The evolution documented in the Pyrenees, with two magmatic events separated by a compressional episode, argues against a continuous extensional regime related to the opening of the Rheic or the Rheic and Paleotethys oceans during the Ordovician and Silurian.

Acknowledgements

This study was supported by the Spanish Commission for Science and Technology, project CGL-2007-66857CO2-02 and the Consolider-Ingenio 2010 programme, under CSD2006-00041 "Topoiberia". We would like to thank the SUMAC staff at Stanford University, especially Joe Wooden and Ariel Strickland, for their help in operating the SHRIMP instrument and in interpreting the results. P. Castiñeiras's time at the SUMAC facility was funded by a "Profesores UCM en el extranjero" travel grant. Detailed comments of three anonymous referees and D. Nance have greatly enhanced the original version of the manuscript.

Appendix A. Supplementary data

Supplementary data associated with this article can be found, in the online version, at doi:10.1016/j.gr.2009.10.006.

References

Abad, A., 1987. Primera cita de arqueociátidos en Cataluña. Trabajos Museo Geología Seminario Barcelona 222, 10.

Alias, G., Casas, J.M., Cirés, J., Liesa, M., 2000. The large-scale structure of the Canigó Massif (Eastern Pyrenees) implications for the Hercynian tectonics. 15th International Conference on Basement Tectonics. A Coruña, Spain.

Autran, A., Fonteilles, M., Guitard, G., 1970. Relations entre les intrusions de granitoides, l'anatexie, et le métamorphisme régional considerées principalment du point de vue de l'eau: cas de la Chaine hercynienne des Pyrénées Orientales. Bulletin Societé Géologique de France 7, 673–731.

Ayora, C., Casas, J.M., 1986. Strabound As–Au mineralization in pre-Caradocian rocks form the Vall de Ribes, Eastern Pyrenees, Spain. Mineralium Deposita 21, 278–287.

Barnolas, A., García-Sansegundo, J., 1992. Caracterización estratigráfica y estructural del Paleozoico de Les Gavarres (Cadenas Costero Catalanas, NE de España). Boletín Geológico y Minero 103, 94–108.

Bea, F., Montero, P., Talavera, C., Zinger, T., 2006. A revised Ordovician age for the Miranda do Douro orthogneiss, Portugal. Zircon U–Pb ion-microprobe and LA-ICPMS dating. Geologica Acta 4, 395–401.

Black, L.P., Kamo, S.L., Allen, C.M., Davis, D.W., Aleinikoff, J.N., Valley, J.W., Mundil, R., Campbell, I.H., Korsch, R.J., Williams, I.S., Foudoulis, C., 2004. Improved $^{206}Pb/^{238}U$ microprobe geochronology by the monitoring of a trace-element-related matrix effect, SHRIMP, ID-TIMS, ELA-ICP-MS and oxygen isotope documentation for a series of zircon standards. Chemical Geology 205, 115–140.

Calvet, P., Lapierre, H., Charvet, J., 1988. Diversité du volcanisme Ordovicien dans la région de Pierrefitte (Hautes Pyrénées): rhyolites calco-alcalines et basaltes alcalins. Comptes Rendus Académie Sciences Paris 307, 805–8128.

Casas, J.M., 1984. Estudi de la deformació ens els gneiss del massís del Canigó. Ph.D. thesis, Barcelona University.

Casas, J.M., in press. Ordovician deformations in the Pyrenees: new insights into the significance of pre-Variscan ("Sardic") tectonics. Geological Magazine 147. doi:10.1017/S0016756809990756.

Casas, J.M., Fernández, O., 2007. On the Upper Ordovician unconformity in the Pyrenees: new evidence from the La Cerdanya area. Geologica Acta 5, 193–198.

Casas, J.M., Fernández, O., 2008. Late Ordovician extensional tectonics in the Eastern Pyreenes. Geo-Temas 10, 213.

Castiñeiras, P., Navidad, M., Liesa, M., Carreras, J., Casas, J.M., 2008a. U–Pb zircon ages (SHRIMP) for Cadomian and Lower Ordovician magmatism in the Eastern Pyrenees: new insights in the pre-Variscan evolution of the northern Gondwana margin. Tectonophysics 461, 228–239.

Castiñeiras, P., Villaseca, C., Barbero, L., Martín Romera, C., 2008b. SHRIMP U–Pb zircon dating of anatexis in high-grade migmatite complexes of Central Spain: implications in the Hercynian evolution of Central Iberia. International Journal of Earth Sciences 97, 35–50.

Cocherie, A., Baudin, Th., Autran, A., Guerra, C., Fanning, C.M., Laumonier, B., 2005. U–Pb zircon (ID-TIMS and SHRIMP) evidence for the early Ordovician intrusion of metagranites in the late Proterozoic Canaveilles Group of the Pyrenees and the Montagne Noire (France). Bulletin Societé Géologique de France 176, 269–282.

Delaperrière, E., Lancelot, J., 1989. Datation U–Pb sur zircons de l'orthogneiss du Capo Spartivento (Sardaigne, Italie), nouveau témoin d'un magamatisme alcalin ordovicien dans le sud de l'Europe. Comptes Rendus Académie Sciences Paris 309, 835–842.

Delaperrière, E., Soliva, J., 1992. Détermination d'un âge Ordovicien supérieur–Silurien des gneiss de Casemi (Massif du Caigou, Pyrénées Orientales) par la méthode

d'évaporation du plomb sur monozircon. Comptes Rendus Académie Sciences Paris 314, 345–350.

Denele, Y., Barbey, P., Deloule, E., Pelleter, E., Olivier, Ph., Gleizes, G., 2009. Middle Ordovician U–Pb age of the Aston and Hospitalet orthogneissic laccoliths: their role in the Variscan evolution of the Pyrenees. Bulletin Societé géologique de France 180, 209–221.

Díez Montes, A., Martínez Catalán, J.R., Bellido Mulas, F., 2010. Role of the Ollo de Sapo massive felsic volcanism of NW Iberia in the Early Ordovician dynamics of northern Gondwana. Gondwana Research 17 (2–3), 363–376 (this issue).

Finney, S., 2005. Global series and stages for the Ordovician system. A progress report. Geologica Acta 3, 309–316.

Fontboté, J.M., Guitard, G., 1958. Aperçus sur la tectonique cassante de la zone axiale dels Pyrénées orinentales entre les bassins de la Cerdagne et de l?ampurdan-Roussillon. Bulletin Societé Géologique de France 8, 884–890.

Franz, L., Romer, R.L., 2007. Caledonian high-pressure metamorphism in the Strona–Ceneri-Zone (Southern Alps of southern Switzerland and northern Italy). Swiss Journal of Geosciences 100, 457–467.

Guillot, F., Schaltegger, U., Bertrand, J.M., Deloule, E., Baudin, T., 2002. Zircon U–Pb geochronology of Ordovician magmatism in the polycyclic Ruitor Massif (Internal W-Alps). International Journal of Earth Sciences 91, 964–978.

Guitard, G., 1953. La structure du massif du Canigou. Bulletin Societé Géologique de France 3, 907–924.

Guitard, G., 1970. Le métamorphisme hercynien mésozonal et les gneiss oeillés du massif du Canigou (Pyrénées-Orientales). Mémoire Bureau Recherches Géologiques et Minières 63.

Guitard G., Laumonier B., Autran A., Bandet Y., Berger G.M., 1998. Notice explicative, Carte géologique France (1:50.000), feuille Prades (1095). Orléans, Bureau Recherches Géologiques et Minières.

Handy, M.R., Franz, L., Heller, F., Janott, B., Zurbriggen, R., 1999. Multistage accretion and exhumation of the continental crust (Ivrea crustal section, Italy and Switzerland). Tectonics 18, 1154–1177.

Helbing, H., Tiepolo, M., 2005. Age determination of Ordovician magmatism in NE Sardinia and its bearing on Variscan basement evolution. Journal of the Geological Society of London 162, 689–700.

Ireland, T.R., Williams, I.S., 2003. Considerations in zircon geochronology by SIMS. In: Hanchar, J.M., Hoskin, P.W.O. (Eds.), zircon. Reviews in Mineralogy and Geochemistry, vol. 53. Mineralogical Society of America, Washington, pp. 215–241.

Laumonier, B., 1988. Les groupes de Canaveilles et de Jujols («Paléozoïque inférieur») des Pyrénées orientales. Arguments en faveur de l'âge essentiellement cambrien de ces séries. Hercynica 4, 25–38.

Laumonier, B., Autran, A., Barbey, P., Cheilletz, A., Baudin, Th., Cocherie, A., Guerrot, C., 2004. Conséquences de l'absence de socle cadomien sur l'âge et la signification des séries pré-varisques (anté-Ordovicien supérieur) du sud de la France (Pyrénées, Montagne Noire). Bulletin Societé Géologique de France 175, 643–655.

Liesa, M., Carreras, J., Castiñeiras, P., Navidad, M., Casas, J.M., Vilà. M., in press. U–Pb zircon age of Prevariscan rocks of the Albera Massif (Pyrenees). Acta 8.

Ludwig, K.R., 1998. On the treatment of concordant uraniumlead ages. Geochimica et Cosmochimica Acta 62, 665–676.

Ludwig, K.R., 2002. SQUID 1.02, A User's Manual: Berkeley Geochronology Center Special Publication, vol. 2. 17 pp.

Ludwig, K.R., 2003. ISOPLOT/Ex, version 3, A Geochronological Toolkit for Microsoft Excel: Berkeley Geochronology Center Special Publication, vol. 4. 71 pp.

Ludwig, K.R., Turi, B., 1989. Paleozoic age of the Capo Spartivento Orthogneiss, Sardinia, Kitaly. Chemical Geology 79, 147–153.

Marini, F., 1988. "Phase" sarde et distension ordovicienne du domaine sud-varisque, effets d'un pont chaud? Une hypothèse fondée sur les données nouvelles du volcanisme albigeois. Comptes Rendus Académie Sciences Paris 306, 443–450.

Martí, J., Muñoz, J.A., Vaquer, R., 1986. Les roches volcaniques de l'Ordovicien supérieur de la région de Ribes de Freser-Rocabruna (Pyrénées catalanes): caractères et signification. Comptes Rendus Académie Sciences Paris 302, 1237–1242.

Maurel, O., Brunel, M., Monié, P., 2002. Exhumation cénozoïque des massifs du Canigou et de Mont-Louis (Pyrénées Orientales, France). Comptes Rendus Geoscience 334, 941–948.

Murphy, J.B., Gutiérrez-Alons, oG., Fernández-Suárez, J., Braid, J.A., 2008. Probing crustal and mantle lithosphere origin through Ordovician volcanic rocks along the Iberian passive margin of Gondwana. Tectonophysics 461, 166–180.

Navidad, M., Barnolas, A., 1991. El magmatismo (Ortogneises y volcanismo del Ordovícico Superior) del Paleozoico de los Catalanides. Boletín Geológico y Minero 102, 187–202.

Navidad, M., Casas, J.M., Castiñeiras, P., Barnolas, A., Fernández-Suárez, J., Liesa, M., Carreras, J., Gil-Peña, I., 2010. Geochemical characterization and isotopic age of the Caradocian magmatism from North-Eastern Iberian Peninsula: Insights from the late Ordovician evolution of the northern Gondwana margin. Gondwana Research 17 (2–3), 325–337 (this issue).

Oggiano, G., Gaggero, L., Funedda, A., Buzzi, L., Tiepolo, M., 2010. Multiple early Paleozoic volcanic events at the northern Gondwana margin: U–Pb age evidence from the Southern Variscan branch (Sardinia, Italy). Gondwana Research 17 (1), 44–58 (this issue).

Pidgeon, R.T., Furfaro, D., Kennedy, A.K., Nemchin, A.A., van Bronswjk, W., 1994. Calibration of zircon standards for the Curtin SHRIMP II. U.S. Geological Survey Circular 1107, 251.

Pin, C., Marini, F., 1993. Early Ordovician continental break-up in Variscan Europe: Nd-Sr isotope and trace element evidence from bimodal igneous associations of the Southern Massif central, France. Lithos 29, 177–196.

Ravier, J.R., Thiébaut, J., Chevenoy, M., 1975. Sur l'importance des évenéments calédoniens dans l'histoire de la chaîne pyrénéenne. Comptes Rendus Académie Sciences Paris 280, 2521–2523.

Robert, J.F., Thiebaut, J., 1976. Découverte d'un volcanisme acide dans le Caradoc de la région de Ribes de Feser (Prov. de Gerone). Comptes Rendus Académie Sciences Paris 282, 2050–2079.

Roger, F., Respaut, J.P., Brunel, M., Matte, Ph., Paquette, J.L., 2004. Première datation U–Pb des orthogneiss oeillés de la zone axiale de la Montgane Noire (Sud du Massif central): nouveaux témoins du magmatisme ordovicien dans la chaîne varisque. Comptes Rendus Geoscience 336, 19–28.

Santanach, P., 1972. Estudio tectónico del Paleozoico inferior del Pirineo entre la Cerdaña y el río Ter. Acta Geológica Hispánica 7, 44–49.

Schaltegger, U., Abrecht, J., Corfu, F., 2003. The Ordovician orogeny in the Alpine basement: constraints from geochronology and geochemistry in the Aar Massif (Central Alps). Schweizerische Mineralogische und Petrologische Mitteilungen 83, 183–195.

Stacey, J.S., Kramers, J.D., 1975. Approximation of terrestrial lead isotope evolution by a two-stage model. Earth and Planetary Science Letters 26, 207–221.

Stampfli, G.M., Von Raumer, J.F., Borel, G.D., 2002. Paleozoic evolution of pre-Variscan terranes: from Gondwana to the Variscan collision. In: Martínez Catalán, J.R., Hatcher, R.D., Arenas, R., Díaz García, F. (Eds.), Special Paper, vol. 364. Geological Society of America, Boulder, Colorado, pp. 263–280.

Talavera, C., Bea, F., Montero, P., Whitehouse, M., 2008. A revised Ordovician age for the Sisargas orthogneiss, Galicia (Spain). Zircon U–Pb ion-microprobe and LA-ICPMS dating. Geologica Acta 6, 313–317.

Trombetta, A., Cirrincione, R., Corfú, C., Mazzoleni, P., Pezzino, A., 2004. Mid-Ordovician U–Pb ages of porphyroids in the Peloritan Mountains (NE Sicily): palaeogeographical implications for the evolution of the Alboran microplate. Journal of the Geologica Society, London 161, 265–276.

Valverde-Vaquero, P., Dunning, G.R., 2000. New U–Pb ages for Early Ordovician magmatism in Central Spain. Journal of the Geological Society of London 157, 15–26.

Vialette, Y., Casquet, C., Fuster, J.M., Ibarrola, E., Navidad, M., Peinado, M., Villaseca, C., 1987. Geochronological study of orthogneisses from the sierra de Guadarrama (Spanish Central System). Neues Jahrbuch Fur Mineralogie. Abhandlungen 10, 465–479.

Von Raumer, J.F., Stampfli, G.M., Borel, G., Busy, F., 2002. Organization of pre-Variscan basement areas at the north-Gondwanan margin. International Journal of Earth Sciences 91, 35–52.

Williams, I.S., 1997. U–Th–Pb geochronology by ion microprobe: not just ages but histories. Economic Geology 7, 1–35.

Zeck, H.P., Whitehouse, M.J., Ugidos, J.M., 2007. 496± 3 Ma zircon ion microprobe age for pre-Hercynian granite, Central Iberian Zone, NE Portugal (earlier claimed 618 ± 9 Ma). Geological Magazine 144, 21–31.

Zurbriggen, R., Franz, L., Handy, M.R., 1997. Pre-Variscan deformation, metamorphism and magmatism in the Strona–Ceneri Zone (southern Alps of northern Italy and southern Switzerland). Schweizerische Mineralogische und Petrologische Mitteilungen 77, 361–380.

Zwart, H.J., 1979. The geology of the Central Pyrenees. Leidse Geologische Mededelingen 50, 1–74.